

COVID-19 Detection Using Segmentation, Region Extraction and Classification Pipeline

Kenan Morani

kenan.morani@gmail.com, 0000-0002-4383-5732

Electrical and Electronics Engineering Department, Izmir Democracy University, Izmir, Turkey

ABSTRACT

Purpose

The main purpose in this study is to propose a pipeline for COVID-19 detection from a big and challenging database of Computed Tomography (CT) images. The proposed pipeline includes a segmentation part, a region of interest extraction part, and a classifier part.

Methods

The methodology used in the segmentation part is traditional segmentation methods as well as UNet based segmentation. In the classification part a Convolutional Neural Network (CNN) was used to take the final diagnosis decisions.

Results

In the segmentation part, the proposed segmentation methods show high dice scores on a publicly available dataset. In the classification part, the results show high accuracy on the validation partition of COV19-CT-DB dataset as well as higher precision, recall, and macro F1 score. The classification results were compared to our previous works other studies as well as on the same dataset.

Conclusions

The improved work in this paper proposes efficient pipeline with a potential of having clinical usage for COVID-19 detection and diagnosis via CT images.

The code is on github at https://github.com/IDU-CVLab/COV19D_3rd

Keywords— *Segmentation, Dice Score, Lung Extraction, Classification, Computed Tomography, Macro F1 Score*

1. INTRODUCTION

COVID-19 affects different people in different ways. Most infected people will develop mild to moderate illness and recover without hospitalization. Most common symptoms of COVID-19 are fever, cough, tiredness, and loss of smell. The virus has been spreading since its onset at the end of 2019. Globally, as of 28 September 2022, there have been 613,410,796 confirmed cases of COVID-19, including 6,518,749 deaths, reported to World Health Organization (WHO). As of September 2022, a total of 12,659,951,094 vaccine doses have been administered [1].

Chest CT scan remains the most sensitive imaging modality in initial diagnosis and management of suspected and confirmed patients with COVID-19. Other diagnostic imaging modalities could add value in evaluating disease progression and monitoring critically ill patients with COVID-19 [2].

In this paper, a pipeline of CT images segmentation, lung area extraction, and classification for COVID-19 detection is proposed. This pipeline has potentials to be deployed for clinical usages.

2. RELATED WORK

A lot of research has been done in the area of medical image segmentation and classification. Many researchers used the publicly available dataset ‘COVID-19 CT segmentation dataset’ [3] for segmentation tasks. Similarly, the private COV19-CT-DB database [4, 5, 6, 7, 8, 9] was also used by many researchers for the purpose of COVID-19 diagnosis and detection.

One research work introduced “inf-Net” method as an automated COVID-19 lung infection segmentation including ‘COVID-19 CT segmentation dataset’. The proposed neural network aimed to automatically identify infected regions from chest CT scans. The proposed Inf-Net was found to outperform most cutting-edge segmentation models and advances the state-of-the-art performance. The reported Dice score was 0.682 [10].

Another work on the same dataset proposed a method called ‘D2A U-Net:’ as an automated segmentation solution with dilated Convolution and Dual Attention mechanism. The proposed method outperforms cutting edges methods in semantic segmentation. The method with pretrained encoder achieves a Dice score of 0.7298 and recall score of 0.7071 [11].

Higher Dice score on the same dataset was reported at [12]. The proposed method was a residual attention U-Net for automated multi-class segmentation of COVID-19 infection region. The study provided a promising deep leaning-based segmentation tool to lay a foundation to quantitative diagnosis of COVID-19 lung infection in CT images. The reported dice score was 0.83. Later work improved the dice score to 0.94.

In classification-oriented work on COV19-CT-DB dataset, one paper [13] presented a transformer-based framework for automatic COVID19 diagnosis. The framework in the paper consisted of two main stages: lung segmentation using UNet followed by the classification. The evaluation results show that the method with the backbone of Swin transformer gain the best F1 score of 0.935 on the validation dataset. The final prediction model with Swin transformer achieves the F1 score of 0.84 on the test dataset.

Our work in here proposed a pipeline of segmentation, lung extraction, and classification. Our method better locates lung region of interest using pretrained UNet segmentation model and approach the classification task from the prospective of looking at representative areas of the slices. In that, it combines the work of the authors mentioned above on the same datasets.

3. DATASET

The dataset used in this paper is an extension of the COV19-CT-DB database, which includes annotated CT scans of 1,650 COVID and 6,100 Non-COVID cases. The annotation was performed by experts of more than 20 years (4 of them). Each CT scan includes between 50 to 700 slices. In here, we use the original training set and part of the original validation set (partition) of it. The dataset is provided via the “ECCV 2022: 2nd COV19D Competition” [14].

The training set contains, in total, 1992 CT scans and the validation set consists of 494 CT scans. The number of COVID-19 and of Non-COVID-19 cases in each set are shown in Table 1. Furthermore, the number of CT scans in the test set is 5281.

Table 1 Distribution of cases in training and validation partitions

Annotation	Training Data	Validation Data
COVID-19 cases	882	215
Non-COVID cases	1110	269 out of 289

4. METHODOLOGY

The methodology includes a workflow starting with segmentation, lung extraction, and finishing with a classification model.

The work was entirely implemented on a workstation using GNU/Linux operating system on 64GiB System memory with Intel(R) Xeon(R) W-2223 CPU @ 3.60GHz processor.

4.1 Segmentation Part

Traditional segmentation methods as well as UNet architecture-based segmentation were used, and their performances were compared in terms of dice similarity. Region based, thresholding-using-Otsu-method based, and clustering with $k=2$ based segmentation methods were used. Moreover, UNet model architecture with 3-level depth was used for segmentation. The results of all these methods were evaluated and compared using the publicly available 'COVID-19 CT segmentation dataset' [3]. From the dataset, only the "Image volumes (308 Mb)", and the "Lung masks (1 Mb)" were used. The slices used for evaluation are the "Lung masks" which were sliced in Z-axial direction and the "Image Volumes" sliced in Z-axial direction. The resulting slices were then segmented using one of the proposed segmentation methods.

The training set included all t2 to t8 images and their corresponding masks; i.e. 745 annotated images and 745 annotated masks. Whereas the test set included all t0 and t1 images and corresponding masks; i.e. 84 annotated images and 84 annotated masks.

The resulting volume slices were compared against the corresponding lung masks in terms of the dice Coefficient value for two classes. Average dice value and minimum dice value over all test lung mask slices were used to evaluate the segmentation performance. The input images were all grayscale, 224x224 sized.

4.1.1 Traditional Segmentation methods

The traditional methods used were region-based, histogram thresholding via otsu, and k-means clustering based with two clusters [15].

4.1.2 UNet based segmentation

The UNet segmentation method included UNet model with different depth levels and existence of batch normalization technique. The UNet model included level depth two and three level depth. The three-level depth was tried without batch normalization and with batch normalization. It was found to perform better with batch normalization. Following that, and in an attempt to check whether the model was too complex a two level UNet model was tried with batch Normalization and the performance was found to be the highest.

For training the UNet model, the following augmentation techniques were applied on the training set:

- Feature wise centering
- Feature wise standard normalization
- Rotation range of 90 degrees
- Width shift and height shift of 0.2
- Zoom range of 0.3

Since various augmentation methods were deployed on the training set, the training epoch steps were chosen as in Equation (1):

$$\text{Training epoch step} = \frac{6 \times \text{number of training set}}{\text{training batch size}} \quad (1)$$

Where *number of training set* = 745 and *training batch size* = 32

As for the test set epoch, Equation (2) depicts the value:

$$\text{Test epoch step} = \frac{\text{number of training set}}{\text{training batch size}} \quad (2)$$

Where *number of test set* = 48 and *test batch size* = 32

In addition, the learning rate was decreased exponentially over the training epochs as in equation (3):

$$\text{New Learning Rate} = \text{Initial Learnin Rate} \times e^{-\text{epoch}} \quad (3)$$

Where *Initial Learnin Rate* = 0.1 and the number of training epochs was 20.

Furthermore, the ‘Adam’ optimizer and “Binary Cross Entropy” loss function were deployed.

4.2 Lung Extraction Part

All the images in the COV19-CT-DB dataset were resized to 224x224 from the original size of 512x512, and all images were converted into grayscale. In order for the pixel intensity range in the COV19-CT-DB images to be similar to the pixel intensity in the public dataset used for segmentation model building the sections above, the pixel intensity values were squeezed to values between 0 and 100 using equation (4):

$$\text{COV19 – CT – DB image pixel intensity} = \frac{\text{original intenisity} \times 100.0}{255.0} \quad (4)$$

The above saved UNet models were used for lung-region extraction from the slices in the COV19-CT-DB database. The “predict” function was used on all the slices in the COV19-CT-DB to result in masks. Those resulting masks were overlaid on their original images to extract the lung regions. This overlaying processing resulted after the following processes:

Border clearness (*border_clear*), binary erosion with “disk (2)”, binary closing with “desk (10)”, edges detection using roberts filter, and filling the holes using “*ndi.binary_fill_holes*”. Finally, the masks were overlaid on the original images using OpenCV “*bitwise_and*”.

4.3 Classification Part

The resulted lung extracted images were used as input to a classifier. The classifier is a convolutional neural network model with four similar hidden layer and a fully connected layer [16].

Both vertical and horizontal flipping were used to achieve data augmentation.

Four 2D convolutional layers with 3x3 filter size, padding=‘same’, batch norm, ReLU activation, and 2D max pooling of size 2x2. The filter size sequenced over the four layers as follows; 16, 32, 64, and 128. These layers were followed by a fully connected layer, which includes flatten layer, dense(256), batch norm, ReLU activation, and drop out of 10%. The output is a dense(1) with sigmoid activation function. The output of the final layer is the class probability for predicting a slice as Non-COVID.

To compile the model, binary cross entropy loss, Stochastic Gradient Decent (SDG) optimizer, and a learning rate scheduler were deployed. The learning rate schedule decreased in an exponential decay during the training, with initial value of 0.1.

5. PERFORMANCE EVALUATION

The matrix used for evaluating the above-mentioned methods were different between segmentation evaluation and classification performance evaluation. For segmentation evaluation, dice similarity score was used. Average dice score and minimum dice score on the test set slices, which are numbered 84 slices, were used [17]. Those scores were evaluated on the test set allocated manually from the publicly available dataset set as mentioned in the segmentation part section above. For the classification part, the macro F1 score was mainly used for performance evaluation [18].

6. RESULTS

The results are discussed in three separate sections; the segmentation results, the Lung extraction results, and the classification results. The segmentation part was validated on the publicly available dataset 'COVID-19 CT segmentation dataset', while the lung extraction and classification results were validated on the private database 'COV19-CT-DB'.

4.1 Segmentation comparison results

Table 2 shows the segmentation results on the 'COVID-19 CT segmentation dataset'. The average dice scores can be compared on the test partition images as well as the minimum dice score. The dataset was used as explained in the segmentation section above. The scores are measured on the test set.

Table 2 Traditional segmentation methods and UNet-based segmentation results on 'COVID-19 CT segmentation' test dataset

<i>Segmentation Method</i>	<i>Average Dice Score</i>	<i>Minimum Dice Score</i>
Region-based	0.8931	0.7450
Histogram-threshold (otsu) based	0.8937	0.7511
k-means clustering (k=2)	0.8938	0.7512
UNet_model (3Layer Depth)	0.9680	1
UNet_model (3Layer Depth & BatchNorm)	0.9760	0.9330

The results show that the UNet mode with three layers in depth and batch Normalization shows the best performance.

4.2 Lung Extraction results

Fig. 1 shows the resulting lung extracted images. Results are randomly picked from CT scan#50 of the COVID, training set.

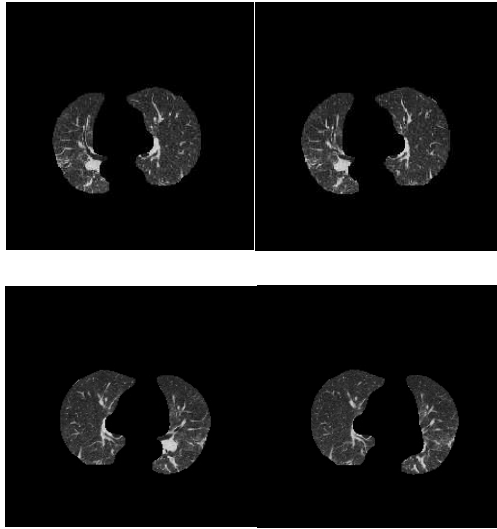


Fig. 1 Lung Extracted slices - COVID slices from the training set

4.4 Classification results

Classification - UNet_model (3-Level Depth) with a CNN model performance result at slices level is shown in Table 3. The table also shows the results for UNet model (3-level depth with batchnorm) at slices level.

Table 3 Classification - UNet_model (3-Level Depth) at slices level

	UNet_model (3-Level Depth)	UNet_model (3-Level Depth and batch Norm)
Macro F1 score	0.764	0.802
Average Precision	0.8	0.758
Average Recall	0.731	0.852

The results show that adding batch norm to the UNet model will increase macro F1 score at the slices level.

To further validate the results, the confidence interval for the resulting macro F1 score, as in equation (5), was used. In the equation, z is taken as $z=1.96$ for a significance level of 95%. By that we can calculate the confidence interval for the macro F1 score (0.802):

$$interval = 1.96 \times \sqrt{\frac{0.802(1 - 0.802)}{106378}} \approx 0.002 \quad (5)$$

The number of samples (slices) in the validation set is 106,378. The result from the last equation shows sufficient confidence in the resulting macro F1 score, i.e. the macro f1 score can be said to be 0.802 ± 0.002 .

The results at patient level using majority voting, with different class probability thresholds, are show in Fig. 4. The figure shows the results for UNet model with and without batch normalization.

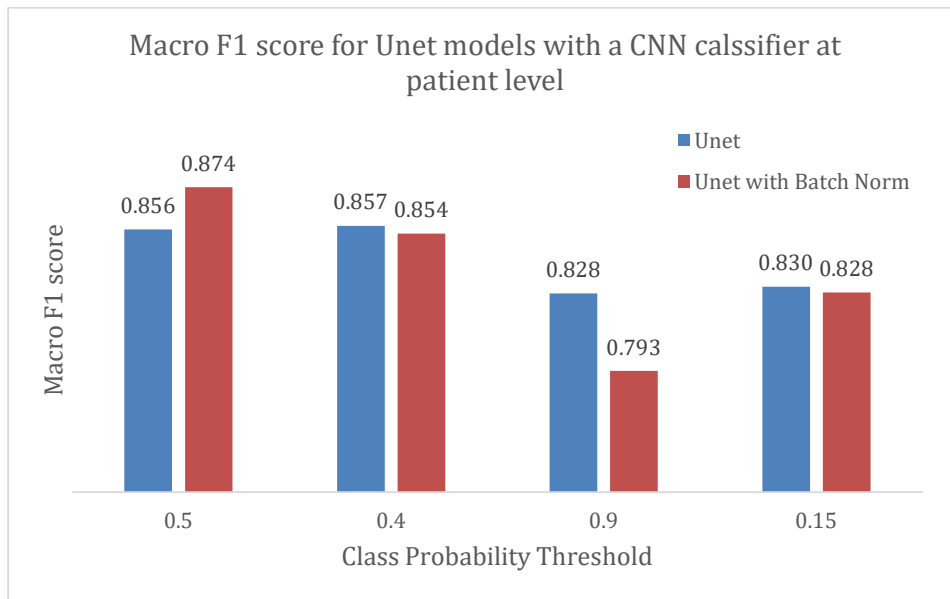


Fig. 2 Macro F1 score at patient level for the pipeline with UNet mode and CNN classifier for different class probability thresholds – the validation set

The results show that using a 0.5 threshold for a UNet model with batch normalization gives the highest macro F1 score at patient level on the validation set of the COV19-CT-DB database.

The improvement achieved comparing to our previous papers at patient level were sufficient in terms of macro F1. The comparison was made on the validation set [19][20]. Table 4 shows the macro F1 score comparison results and the improvement achieved.

Table 4 Comparing the proposed method results to our previous results on the validation set of COV19-CT-DB dataset

Comparing to our previous results	Xception Method [13]	Seg-Ext-Classif (with 3-level depth UNet without batchNorm)	Seg-Ext-Classif (with 3-level depth UNet and batchNorm)
Macro F1 score on validation	0.806	0.857	0.874
Validation Accuracy	81.10%	86.16%	87.81%
Improvement Margin for macro F1	-	0.051	0.068

7. CONCLUSION AND FURTHER WORK

In this work, a pipeline for COVID-19 detection via CT images. Different segmentation methods were compared, and a saved UNet model for segmentation was used for lung extraction from the CT scan images. The resulting images were used as input for a CNN classifier to take diagnosis decision. The results on the validation set seems promising.

Further work focuses on non-representative slice removal techniques. The work will include statistical-based and/or automated machine learning based slice removal techniques to remove uppermost and mower most slices on the CT scan images.

ACKNOWLEDGEMENT

Acknowledgement goes for the medical staff who worked on annotating COVID-CT-DB database and other members who shared the dataset. Acknowledgement to Izmir Democracy University, for provide the c

There is no conflict of interest, and the research received no funds.

REFERENCES:

1. <https://covid19.who.int/> {Last Access 28.09.2022}
2. Aljondi, Rowa, and Salem Alghamdi. "Diagnostic Value of Imaging Modalities for COVID-19: Scoping Review." *Journal of medical Internet research* vol. 22,8 e19673. 19 Aug. 2020, doi:10.2196/19673
3. <http://medicalsegmentation.com/covid19>
4. Kollias, D., Arsenos, A. and Kollias, S., 2022. Ai-mia: Covid-19 detection & severity analysis through medical imaging. arXiv preprint arXiv:2206.04732.
5. Kollias, D., Arsenos, A., Soukissian, L. and Kollias, S., 2021. Mia-cov19d: Covid-19 detection through 3-d chest ct image analysis. In *Proceedings of the IEEE/CVF International Conference on Computer Vision* (pp. 537-544).
6. Kollias, D., Bouas, N., Vlaxos, Y., Brillakis, V., Seferis, M., Kollia, I., Sukissian, L., Wingate, J. and Kollias, S., 2020. Deep transparent prediction through latent representation analysis. arXiv preprint arXiv:2009.07044.
7. Kollias, D., Vlaxos, Y., Seferis, M., Kollia, I., Sukissian, L., Wingate, J. and Kollias, S., 2020, September. Transparent adaptation in deep medical image diagnosis. In *International Workshop on the Foundations of Trustworthy AI Integrating Learning, Optimization and Reasoning* (pp. 251-267). Springer, Cham.
8. Kollias, D., Tagaris, A., Stafylopatis, A., Kollias, S. and Tagaris, G., 2018. Deep neural architectures for prediction in healthcare. *Complex Intell Syst* 4: 119–131.
9. Arsenos, A., Kollias, D. and Kollias, S., 2022, June. A Large Imaging Database and Novel Deep Neural Architecture for Covid-19 Diagnosis. In *2022 IEEE 14th Image, Video, and Multidimensional Signal Processing Workshop (IVMSP)* (pp. 1-5). IEEE.
10. Fan, Deng-Ping, et al. "Inf-net: Automatic covid-19 lung infection segmentation from ct images." *IEEE Transactions on Medical Imaging* 39.8 (2020): 2626-2637.
11. Zhao, Xiangyu, et al. "D2a u-net: Automatic segmentation of covid-19 lesions from ct slices with dilated convolution and dual attention mechanism." arXiv preprint arXiv:2102.05210 (2021).
12. Chen, Xiacong, Lina Yao, and Yu Zhang. "Residual attention u-net for automated multi-class segmentation of covid-19 chest ct images." arXiv preprint arXiv:2004.05645 (2020).
13. Zhang, Lei, and Yan Wen. "A transformer-based framework for automatic COVID19 diagnosis in chest CTs." *Proceedings of the IEEE/CVF International Conference on Computer Vision*. 2021.
14. <https://mlearn.lincoln.ac.uk/eccv-2022-ai-mia/>
15. Pham, Dzung L., Chenyang Xu, and Jerry L. Prince. "A survey of current methods in medical image segmentation." *Annual review of biomedical engineering* 2.3 (2000): 315-337.
16. Morani, Kenan, and Devrim Unay. "Deep Learning Based Automated COVID-19 Classification from Computed Tomography Images." arXiv preprint arXiv:2111.11191 (2021).
17. Zou, Kelly H et al. "Statistical validation of image segmentation quality based on a spatial overlap index." *Academic radiology* vol. 11,2 (2004): 178-89. doi:10.1016/s1076-6332(03)00671-8
18. Opitz, Juri, and Sebastian Burst. "Macro f1 and macro f1." arXiv preprint arXiv:1911.03347 (2019).
19. Morani, Kenan, and Devrim Unay. "Deep Learning Based Automated COVID-19 Classification from Computed Tomography Images." arXiv preprint arXiv:2111.11191 (2021).
20. Morani, Kenan et al. "COVID-19 Detection Using Transfer Learning Approach from Computed Tomography Images." (2022).